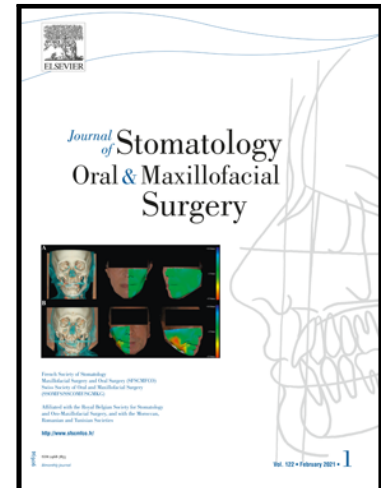


Journal Pre-proof

Intentional craniofacial remodelling in Europe in the XIXth century: quantitative evidence of soft tissue modifications from Toulouse, France

Leila Galiay , Raphaël Cornette , Laura Laliève ,
Quentin Hennocq , Connor Cross , Ali Alazmani ,
Mehran Moazen , Roman Hossein Khonsari

PII: S2468-7855(22)00133-1
DOI: <https://doi.org/10.1016/j.jormas.2022.05.002>
Reference: JORMAS 1186



To appear in: *Journal of Stomatology oral and Maxillofacial Surgery*

Received date: 14 November 2021
Accepted date: 3 May 2022

Please cite this article as: Leila Galiay , Raphaël Cornette , Laura Laliève , Quentin Hennocq , Connor Cross , Ali Alazmani , Mehran Moazen , Roman Hossein Khonsari , Intentional craniofacial remodelling in Europe in the XIXth century: quantitative evidence of soft tissue modifications from Toulouse, France, *Journal of Stomatology oral and Maxillofacial Surgery* (2022), doi: <https://doi.org/10.1016/j.jormas.2022.05.002>

This is a PDF file of an article that has undergone enhancements after acceptance, such as the addition of a cover page and metadata, and formatting for readability, but it is not yet the definitive version of record. This version will undergo additional copyediting, typesetting and review before it is published in its final form, but we are providing this version to give early visibility of the article. Please note that, during the production process, errors may be discovered which could affect the content, and all legal disclaimers that apply to the journal pertain.

© 2022 Published by Elsevier Masson SAS.

Intentional craniofacial remodelling in Europe in the XIXth century: quantitative evidence of soft tissue modifications from Toulouse, France

Leila **Galiay** (1), Raphaël **Cornette** (2), Laura **Laliève** (1), Quentin **Hennocq** (1), Connor **Cross** (3), Ali **Alazmani** (4), Mehran **Moazen** (3), Roman Hossein **Khonsari** (1)

1. Service de chirurgie maxillo-faciale et chirurgie plastique, Hôpital Universitaire Necker – Enfants Malades, Assistance Publique – Hôpitaux de Paris ; Centre de Références Maladies Rares Craniosténoses et Malformations Craniofaciales CRANIOST, Filière Maladies Rares TeteCou ; Faculté de Médecine, Université de Paris ; Paris, France
2. Institut de Systématique, Évolution, Biodiversité (ISYEB), Muséum national d'histoire naturelle, Sorbonne Université, École Pratique des Hautes Études, Université des Antilles, CNRS ; Paris, France.
3. Department of Mechanical Engineering, University College London; London, United-Kingdom
4. Institute of Functional Surfaces, School of Mechanical Engineering, University of Leeds; Leeds, United-Kingdom

Keywords artificial skull deformation; intentional skull deformation; morphometric geometrics

Corresponding author.

RH Khonsari, Hôpital Necker – Enfants Malades, 149 rue de Sèvres, 75015 Paris, France

Tel +33171396613 email roman.khonsari@aphp.fr

Abstract

Intentional skull deformations have been practiced by every human population, since the prehistoric times until the XXth century. In Europe, they were specifically prevalent in the region of Toulouse, France. The soft-tissue modifications due to such practices are not well characterized in the literature due to the rarity of photographic data. Most studies on skull deformations are thus based on skeletal remains. Here we performed a controlled geometric morphometric assessment of 31 frontal pictures and 70 lateral pictures of individuals from Toulouse with intentional deformations extracted from two XIXth century historical French photographic archives. We measured the forces exerted on the skull vault by the traditional deformation device from Toulouse using a 3D-printed skull and pressure sensors. We showed that individuals with Toulouse deformations have distinctive facial features, caused by moderate forces exerted on the skull vault. Our results exhibit and quantify for the first time the real face of intentional skull deformations, which are a ubiquitous and distinctive feature of the human species.

Introduction

Intentional skull deformations were practiced worldwide until the beginning of the XXth century, including in Western Europe.¹ France was one of the most active countries for these practices, with the South-Western region of Toulouse being of their epicentres.²⁻⁴ Toulouse deformations (TD) were obtained by banding the head of new-borns immediately after birth and during the first years of life using a standardized set of devices (Figures 1-2).^{5,6} These devices induced deformations characterised by sagittal lengthening of the skull and a posterior forehead tilt (Figure 3), leading to a shape approaching the better-known circumferential deformations^{7,8} reported for instance in Central and South America,⁹⁻¹¹ Central Africa, and Papua New Guinea.¹ TD seem geographically independent from similar practices that developed in Eastern Europe during the Migration Period, between the IVth and the VIth centuries, imported by ethnic groups such as the Huns,¹² and their earliest reports are from the XVIIth century.⁶ Nevertheless, as in most cases of intentional deformations in Europe and beyond, TD most probably date back to end of the Paleolithic.^{13,14} TD were actively practiced in South-Western France until World War I, and disappeared shortly afterwards, due to the combined effects of sanitary campaigns and the modernization of rural areas.⁶

Toulouse deformations were obtained using two pieces of cloth: the headband and the bandeau (Figures 1-2). The deformation process has been reported in details in the XIXth century French medical literature:^{6,15} (1) the initial step consisted in hand-moulding the head of the new born, generally by mid-wives, in order to initiate the shape modification; (2) a piece of flannel was then positioned on the anterior fontanelle; (3) the head band (called 'sarro-cap' in Toulousan dialect) was placed as a hood and tightly banded around the forehead and the occiput using long fabric pieces (approximately 50 cm long) called 'péoulios' in Toulousan dialect; (4) the bandeau (called 'bendel' or 'pountou' in Toulousan dialect) was finally tightly attached over the head band – this bandeau was formed by a central rectangular

piece of 30 cm x 6-7 cm and by two lateral bands of variable length, used to wrap the head in a similar way as the 'péoulios' of the head band. These devices were kept continuously during the 3-4 first years of life in both boys and girls; girls later wore a similar but more elaborate outfit for the rest of their lives (Figure 2).

Intentional skull deformations have been extensively studied, mostly by physical anthropologists working on skeletal remains.^{11,16} Nevertheless, the aesthetic consequences of these practices are little known, and have only been indirectly inferred, for instance based on orbital morphometrics^{16,17} or zygomatic shape assessments.¹⁸

TD are well documented in two collections of anthropological pictures, resulting from the work of Louis Delisle (1836-1911) and Eugène Trutat (1840-1910). The Delisle collection is stored at the Musée du Quai Branly, Paris and available online on the website of the museum. This collection includes 464 photographs taken by Louis Delisle between 1879 and 1894. The Trutat collection is also available online and archived on *Wikimedia Commons* (*Phoebus* project, 2010, Mairie de Toulouse & *Wikimédia France*). This second collection includes 5233 pictures, mostly taken around 1893.

Based on this rich photographic material, we provide the first quantitative assessment of the facial features of individuals with intentional deformations, using geometric morphometrics on frontal and lateral pictures. We describe the precise soft-tissue facial phenotype associated with TD, a specific type of European circumferential deformation, and use a biomechanical model to relate the force intensities causing TD with other physical phenomena known to modify skull shape in new-borns. Our report on intentional European craniofacial remodelling sheds light on a practice generally associated with South-American and Central African cultures, but which appears to be truly ubiquitous as a distinctive feature of our species.

Materials and methods

1. Photographic archives

Delisle and Trutat Collections were screened online based on four inclusion criteria: (1) image of sufficient quality labelled as TD in the catalogue of the collections, (2) strict frontal and lateral incidences, (3) no beard or moustache hiding the contours of the face and/or the lip commissures and (4) free vertex on lateral pictures or tight headband flattening the hair. Furthermore, the online image database of the Musée du Quai Branly (760695 entries) was interrogated using the 'Toulouse' and 'deformation' keywords separately, and selected pictures were screened based on the criteria listed above. Finally, a series of age-matched (elderly individuals) control frontal and lateral pictures were included using Google Images (Google Inc, Mountain View, CA, USA) based on similar criteria.

2. Geometric morphometrics

Sixteen anatomical landmarks on frontal pictures and a set of 100 curve sliding semi-landmarks on lateral pictures were defined in order to model the shape of the face on both incidences¹⁹ and were placed using ImageJ v.1.53a²⁰, by the same author (LL) (Figure 4 and Table 1). Using MorphoJ v.1.06,²¹ a shape Procrustes ANOVA analysis for error measurement of factor repetition was performed to measure the global matching among measurements and confirmed that both anatomical and semi-landmarks could be used for geometric morphometric assessment. Comparative facial morphology between deformed individuals and controls was assessed based on 2D geometric morphometrics²² using R v.1.2²³ for data processing. Landmarks coordinates were superimposed using a Generalized Procrustes Analysis (GPA).²⁴ Coordinates after GPA were assessed using principal component analysis (PCA). Both GPA and PCA were performed using the **gpagen** and **plotTangentSpace** functions of the **geomorph** package.²⁵⁻²⁷ ANalysis Of VAriance

(ANOVAs) were performed considering ‘deformed’ and ‘controls’ as classifiers. Quantitative data were expressed as mean \pm Standard Derivation or median \pm Interquartile range and were compared using Mann-Whitney test or Kruskal-Wallis test for more than 2 groups. $p < 0.05$ was considered as significant.

3. Biomechanical testing

An infant skull previously developed and described in Libby et al. (2017) was used. In brief, the skull had an estimated age of 39-42 weeks of gestation and unknown sex. It was scanned in an X-Tek HMX160 micro-CT scanner (XTek Systems Ltd, Tring, UK) at the University of Hull, UK, at a resolution of 0.132 mm. The resultant two-dimensional images were imported into Avizo (Thermo Fisher Scientific, Waltham, MA, USA) for segmentation. The specimen used to develop the model was loaned from the University of Dundee, UK, and was from an archaeological source (skull ID: SC-108). The segmented skull was 3D-printed (Stratasys Objet 500; Stratasys Ltd, Eden Prairie, MN, USA). The final printed model was made from two materials: (1) rigid juvenile bones (VeroUltraClear, Stratasys Ltd, Eden Prairie, MN, USA), with a tensile strength of 39-43 MPa, and (2) rubber-like sutures (Agilus30, Stratasys Ltd, Eden Prairie, MN, USA) with a tensile strength of 2.4-3.1 MPa.^{28,29}

TD were reproduced using dressing wrapped around the 3D-printed new-born skull. Force sensors (PPS C500, Quadrtec limited, UK) were used to measure the force applied to the anterior, posterior and the lateral sides of the skull with both the bandeau and the head-band (Figure 5). The bandeau and the head band were tightened by one individual and the procedure was repeated three times. The signal, i.e. changes in the voltage due to external forces at the surface of the sensor was acquired at 100 Hz using a custom program written

code in LabVIEW 2013 (National Instruments Corp, Austin, TX, USA). The force sensors were calibrated using a range of known weights prior to their placement.

Journal Pre-proof

Results

1. Photographic data

1.1 Trutat collection

Two photographs from the Trutat Collection out of 5233 pictures were included (N^oMHNT.TIR.POT.04.04b & N^oMHNT.PHa.1521.05.202) after screening using the dedicated *Wikimedia Commons* interface. On the online collection of Musée du Quai Branly, the keyword 'Toulouse' was associated with 172 entries and the keyword 'deformation' was associated with 1051 entries. The screening of these entries led to the inclusion of 10 photographs that had no mention of a photographer but strong similarities with pictures from the Trutat Collection. In fact, two out these 10 pictures from Musée du Quai Branly were the same as the two pictures included above from the Trutat Collection itself: N^oPV0072249 [lateral view only] = N^oMHNT.PHa.1521.05.202 [frontal & lateral views] and N^oPV0072245 [lateral view only] = N^oMHNT.TIR.POT.04.04b [frontal & lateral views]. In total, 2 frontal pictures (2 men) and 10 lateral pictures (9 men and 1 woman) were included from the Trutat Collection directly or from Musée du Quai Branly (and attributed to Trutat by us).

1.2 Delisle collection

Out of the 464 pictures from the Delisle collection stored on the website of Musée du Quai Branly, 29 frontal views (16 men and 13 women) and 60 lateral views (33 men et 27 women) were included (Figures 6-7).

1.3 Control pictures

Control pictures – 40 frontal views (26 men and 14 women) and 65 lateral pictures (36 men and 29 women) – were included using Google Images.

2. Morphometric assessment

The global morphology of individuals with Toulouse deformations was significantly different from controls, both based on frontal ($p=0.008$) and lateral ($p<0.0001$) pictures. PCA then allowed to assess the morphological characteristics accounting for the most significant percentages of the total variance within the sample (controls and deformed skulls).

On frontal pictures, the first principal component (PC1) represented 44.47 % of the variance; the second principal component (PC2) represented 14.97 % of the variance and the third principal component (PC3) represented 9.55 % of the variance. Deformed and control faces were not obviously separated by PC1 (Figure 8). The first canonical axis showed that Toulouse deformation was associated with longer faces and dropping lip commissures (Figure 9). The classification accuracy (Toulouse vs controls) of a frontal picture picked randomly was 91.55%.

On lateral pictures, the first principal component (PC1) represented 69.36 % of the variance; the second principal component (PC2) represented 11.29 % of the variance and the third principal component (PC3) represented 5.56 % of the variance. PC1 clearly separated Toulouse deformations from controls, deformed skulls being segregated in the positive values of this principal component (Figure 10).

3. Biomechanical modelling

Force measurement showed that most of the constraints exerted on the forehead and the occiput are induced by the bandeau rather than by the headband (Figure 11). Here, the forces applied by the bandeau were in the range of 1.3-1.7N while the forces applied by the headband were in the range of 0.1-0.2N. The total forces measured in the anterior and posterior part of the skull (1.7-1.9N) were slightly larger than the lateral forces measured across the temporal bone (1.4-1.7N).

Journal Pre-proof

Discussion and conclusion

This report is the first quantitative assessment of soft-tissue anomalies in intentional craniofacial remodelling. Facial modifications in these deformations had been inferred from various studies on the skeleton, including studies specifically dedicated to TD,¹⁶⁻¹⁸ but never formally demonstrated. In fact, Toulouse deformations have been investigated since the XVIIIth century³⁰⁻³³ with very few quantitative approaches.

TD are associated with skull vault thickness modifications, such as focal thinning in the compression regions and compensatory thickening in adjacent areas.^{6,16} These irregularities may have resulted in a coronal groove mentioned by several authors in the populations of this region in the XIXth and early XXth centuries,^{6,34} even though this anomaly was not found on dry skulls of individuals with Toulouse deformations.¹⁶⁻¹⁸ This coronal groove may have corresponded to the area underlying the bandeau, but could not be obviously noted on the pictures from the Delisle and Trutat collections.

2D and 3D cephalometric approaches have shown that Toulouse deformations induced skull sagittal lengthening and platybasia,³⁵⁻³⁸ similar to what has been reported in circumferential deformations from Central and South America.^{9,10} Platybasia in Toulouse deformations may have been associated with prognathism, as suggested by several authors,^{2,3,15} even though this fact is debated in the literature⁶; more recently, 3D geometric morphometric approaches on a series of 7 skull with Toulouse deformations have shown a trend towards an anterior shift of the glenoid fossa and shorter distances between left and right glenoid fossa, without reaching statistical significance³⁸, which is also in line with prognathism. We limited the assessment of profiles to the forehead and orbito-nasal regions as many individuals had moustaches hiding the upper lip. Answering the question of prognathism in Toulouse deformations would require

cephalometric analyses on skeletal data for which occlusion can be simulated with the remaining teeth, which is a difficult issue as data is scarce and many skulls have partial / total tooth loss.

Morphometric assessments focused on the orbits and the zygoma in TD have shown that the orbital volume was conserved but the orbits were shallow and that the underlying zygoma was tilted backwards, indicating that patients with TD may have presented with a certain degree of exorbitism.¹⁶⁻¹⁸ Pictures from Trutat and Delisle collections were not adapted to assess this point as eye closure was very variable and fine details were blurred, and there is no current data available to answer the question of exorbitism in TD.

In brief, our data indicate clear and specific craniofacial soft-tissue modifications in TD, demonstrating for the first time that subjects with intentional skull deformations had a distinctive face, which is in line with the cultural adhesion to these practices, even at the beginning of the XXth century.

Our biomechanical model showed that forces exerted by deformation devices in TD were about 1.5-2 N in amplitude. The most common cause of head deformation is positional posterior plagiocephaly, due to supine sleep position.³⁹ The average weight at birth is 3.5 kg and the head corresponds to 1/4th of the weight in new-borns: the force exerted on the back of the head of a sleeping new-born is thus about 9 N in magnitude. Our results indicate that much weaker forces can still induce significant skull deformations. Surprisingly, despite the high prevalence of posterior plagiocephaly, and the numerous treatment options involving the application of external mechanical forces (orthoses), few biomechanical simulations of skull deformation after birth are available in the literature.⁴⁰

Using an approach combining morphometrics and biomechanics, we have shown that moderate forces exerted on the skull can induce significant deformations of facial soft tissues.

Intentional deformations are now an extinct practice but their assessment sheds light on the current sources of head deformation. The objective characterisation of facial traits in intentional deformations furthermore underlines the social role of this practice in inducing well-characterized extraordinary artificial features in a population group.

Acknowledgements

Special thanks to Bertrand de Viviés and Françoise & Lucien Sormail for providing information on deformation methods. Thanks to Annabelle Lacour and Philippe Charlier, from Musée du Quai Branly, for helping with the access to the photographic collections. Thanks to Jacques Gélis for providing access to the less accessible references. We also thank Rosetrees Trust (A1899) who supported Moazen and Cross.

References

1. Dingwall EJ. Artificial Cranial Deformation a contribution to the study of ethnic mutilations. Londres: Bale and Danielsson; 1931.
2. Broca P. Sur la déformation toulousaine du crâne. Bull Mem Soc Anthropol Paris 1871;6:100-131.
3. Delisle F. Sur les déformations artificielles du crâne dans les Deux-Sèvres et les Haute-Garonne. Bull Mem Soc Anthropol Paris 1889;12:649-669.
4. Delisle F. Les déformations artificielles du crâne en France. Carte de leur distribution. Bull Mem Soc Anthropol Paris 1902;5: 111-167.
5. Ambialet MJ. La déformation artificielle de la tête dans la région toulousaine. Toulouse: Université de Toulouse; 1893.
6. Gélis J. Refaire le corps : les déformations volontaires du corps de l'enfant à la naissance. Ethnologie Française 1984;14;7-28.

7. Imbelloni J. Die Arten der künstlichen Schädeldeformation. *Anthropos* 1930;25:801-830.
8. Dembo A, Imbelloni J. Deformaciones intencionales del cuerpo humano de caracter etnico. Buenos Aires: Nova; 1938.
9. Anton SC. Intentional cranial vault deformation and induced changes of the cranial base and face. *Am J Phys Anthropol* 1989;79:253-67.
10. Kohn LA, Leigh SR, Jacobs SC, Cheverud JM. Effects of annular cranial vault modification on the cranial base and face. *Am J Phys Anthropol* 1993;90:147-168.
11. Tiesler V. The bioarcheology of artificial cranial modifications. New approaches to head shaping and its meanings in Pre-Columbian Mesoamerica and beyond. New-York: Springer; 2014.
12. Buchet L. La déformation crânienne en Gaule et dans les régions limitrophes pendant le haut Moyen Âge : son origine – sa valeur historique. *Archéologie médiévale* 1988;18:55-71.
13. Durband AC. Artificial cranial deformation in Pleistocene Australians: the Coobool creek sample. *J Hum Evol* 2008;54:795-813.
14. Zhang Q, Liu P, Yeh HY, Man X, Wang L, Zhu H, Wang Q, Zhang Q. Intentional cranial modification from the Houtaomuga Site in Jilin, China: earliest evidence and longest in situ practice during the Neolithic Age. *Am J Phys Anthropol* 2019;169:747-756.
15. Gosse LA. *Essai sur les déformations artificielles du crâne*. Paris: JB Baillière; 1855.
16. Khonsari RH, Friess M, Nysjö J, Odri G, Malmberg F, Nyström I, Messo E, Hirscej JM, Cabanis EAM, Kunzelmann KH, Salagnac JM, Corre P, Ohazama A, Sharpe PT, Charlier P, Olszewski R. Shape and volume of craniofacial cavities in intentional skull deformation. *Am J Phys Anthropol* 2013;151:110-119.

17. Sandy R, Hennocq Q, Nysjö J, Giran G, Friess M, Khonsari RH. Orbital shape in intentional skull deformations and adult sagittal craniosynostosis. *J Anat* 2018;233:302-310.
18. Ketoff S, Girinon F, Schlager S, Friess M, Schouman T, Rouch P, Khonsari RH. Zygomatic bone shape in intentional cranial deformations: a model for the study of interactions between skull growth and facial morphology. *J Anat* 2017;230:524-531.
19. Gunz P, Mitteroecker P. Semilandmarks: a method for quantifying curves and surfaces. *Hystrix, the Italian Journal of Mammalogy*. 2013;24:103-109.
20. Schneider, C. A., Rasband, W. S., & Eliceiri, K. W. (2012). NIH Image to ImageJ: 25 years of image analysis. *Nature methods*, 9, 671-675.
21. Klingenberg CP. MorphoJ: an integrated software package for geometric morphometrics. *Mol Ecol Resour* 2011;11:353-357.
22. Zelditch ML, Swiderski DL, Sheets HD. *Geometric morphometrics for biologists: a primer*. Cambridge: Academic Press, 2012.
23. R Core Team (2019). *R: A language and environment for statistical computing*. R Foundation for Statistical Computing, Vienna, Austria. URL <https://www.R-project.org/>
24. Rohlf FJ, Slice D. Extensions of the Procrustes method for the optimal superimposition of landmarks. *Syst. Zool* 1990;39:40-59.
25. Adams DC, Collyer ML, and Kaliontzopoulou A. 2018. Geomorph: Software for geometric morphometric analyses. R package version 3.0.6. <https://cran.r-project.org/package=geomorph>
26. Bookstein FL. Principal warps: Thin-plate splines and the decomposition of deformations. *IEEE Transactions on pattern analysis and machine intelligence*. 1989;11:567-585.

27. Schlager S. *Morpho and Rvcg - Shape Analysis in R*. In: Zheng G, Li S, Szekely G (eds.). *Statistical Shape and Deformation Analysis*, p. 217-256. Cambridge: Academic Press, 2017.
28. McPherson GK, Kriewall TJ. The elastic modulus of fetal cranial bone: a first step towards an understanding of the biomechanics of fetal head molding. *J Biomech* 1980;13:9-16.
29. Moazen M, Peskett E, Babbs C, Pauws E, Fagan MJ. Mechanical properties of calvarial bones in a mouse model for craniosynostosis. *PLoS One* 2015;10:e0125757.
30. Icart JF. *Leçons pratiques sur l'art des accouchements, destinées à l'instruction des sages-femmes de la province de Languedoc*. Castres: Imprimerie de P.G. de Robert, 1784.
31. Coutelle M. *Observations sur la constitution médicale de l'année 1808 à Albi*. Albi: Baurens et Colassons; 1809.
32. Foville LA. *Influence des vêtements sur nos organes : déformation du crâne résultant de la méthode la plus générale de couvrir la tête des enfants*. Paris: Madame Prevosto-Crocius; 1834.
33. Bérenguer A. *Topographie physique, statistique et médicale du canton de Rabastens*. A. Chauvin & comp., Toulouse, 1850.
34. Gourc H. *Rides occipitales. Stigmate d'hérédité acquise lié à la déformation du crâne dans l'Albigeois*. Thèse, Paris, 1913-1914, №254.
35. Fabié M. *Le crâne toulousain*. Thèse, Toulouse, 1968, №34.
36. Cussenot O, Pereira da Silva M, Martin-Bouyer Y. Modifications of the skull base in artificial deformations of the circumference of the head. *Surg Radiol Anat* 1992 ;14:43-50.
37. Janot F, Strazielle C, Awazu Pereira Da Silva M, Cussenot O. Adaptation of facial

- architecture in the Toulouse deformity. *Surg Radiol Anat* 1993;15:75-76.
38. Cottin M, Khonsari RH, Friess M. Assessing cranial plasticity in humans: the impact of artificial deformation on masticatory and basicranial structures. *C R Acad Sci Paris* 2017;16:545-556.
39. Persing JA. MOC-PS(SM) CME article: management considerations in the treatment of craniosynostosis. *Plast Reconstr Surg* 2008;121;1-11.
40. Keshtgar M. Evaluating the effectiveness of cranial molding for treatment of positional plagiocephaly using finite element analysis. MS, Biomechanical engineering, California Polytechnic State University, San Luis Obispo.

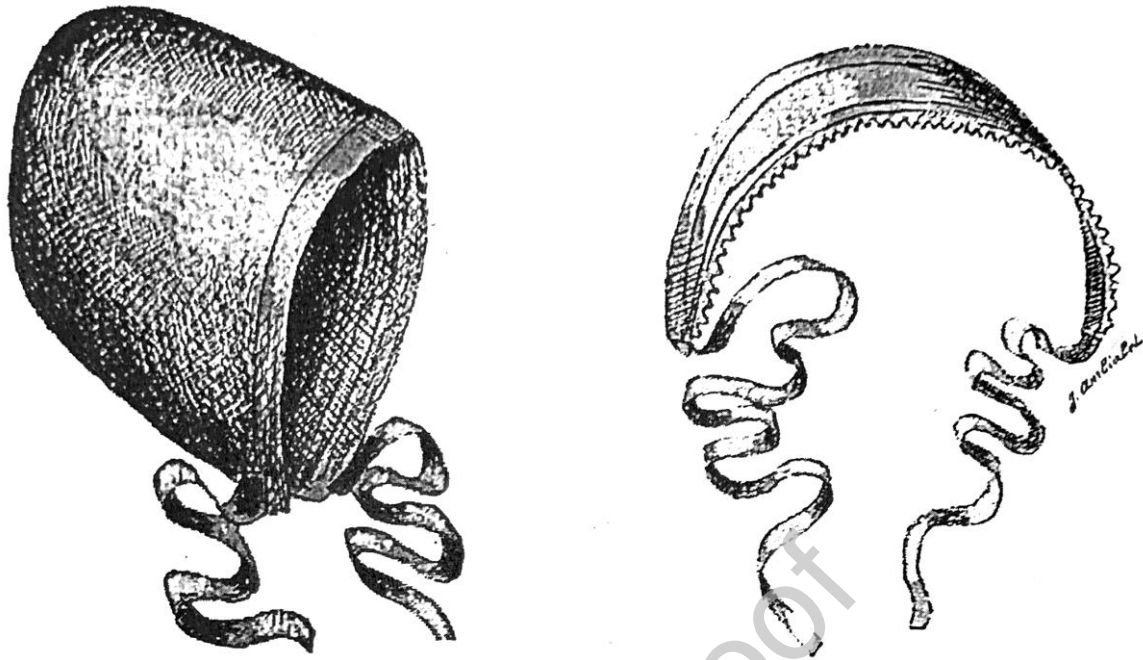


Figure 1. Devices used to induce Toulouse deformations on new-borns: (left) headband ('sarro-cap') with its two bands ('péoulios'); (right) bandeau ('bandel'). After Ambialet 1893.



Figure 2. Traditional Toulouse head dressings worn by Jeanne Beautens, from Fourquevaux (Haute-Garonne, Toulouse region); pictures from the Delisle Collection, 1899. (a, b) bareheaded ; (c, d) headband (black) and two overlapping bandeaus (white); (e) second headband (the 'transparent') covering the first headband and part of the two bandeaus; (f) lace border on the anterior border of the device. After Gélis 1984.



Figure 3. (left) Skull with intentional deformation from the Toulouse region, 65-year-old woman, April 1910, from the Valois collection (№15653); (right) control non-deformed skull. Musée du Quai Branly, №PV0072251.

Journal Pre-proof

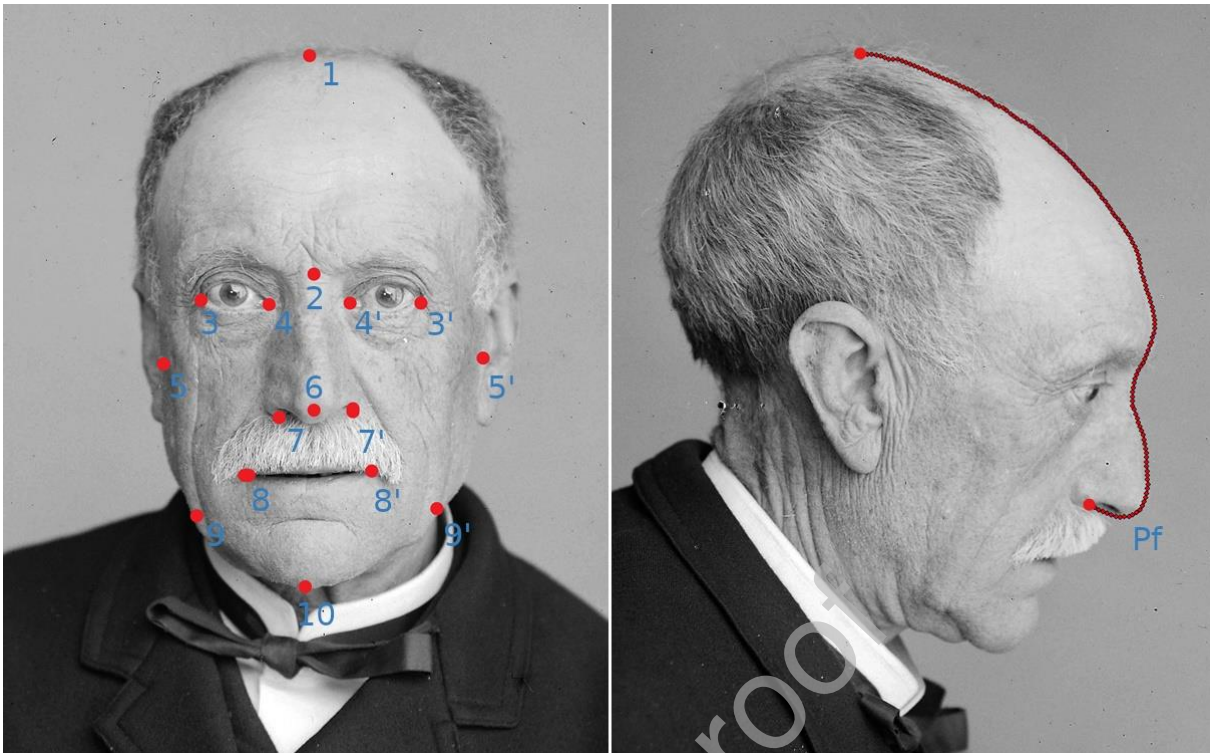


Figure 4. (left) Landmarks used on frontal pictures: (1) forehead top, (2) glabella, (3, 3') external canthus, (4, 4') internal canthus, (5, 5') tracion, (6) nasal prominence, (7, 7') alare, (8, 8') lip commissure, (9, 9') goniac angle, (10) chin; (right) Profile (Pf) outlined from the vertex (in Frankfort orientation) to the columella using 100 sliding landmarks.



Figure 5. Biomechanical modelling of Toulouse deformations using a 3D-printed skull using a bandeau alone (A) and a headband and a bandeau (B).

Journal Pre-proof



Figure 6. Frontal pictures of individuals with intentional deformations from Toulouse region, from the Delisle collection (Musée du Quai Branly, Paris) – 1879-1894 and from the Trutat collection (Muséum d’Histoire Naturelle, Toulouse) – 1859-1910.

Journal Pre-proof



Figure 7. Lateral pictures of individuals with intentional deformations from Toulouse region, from the Delisle collection (Musée du Quai Branly, Paris) – 1879-1894 and from the Trutat collection (Muséum d’Histoire Naturelle, Toulouse) – 1859-1910.

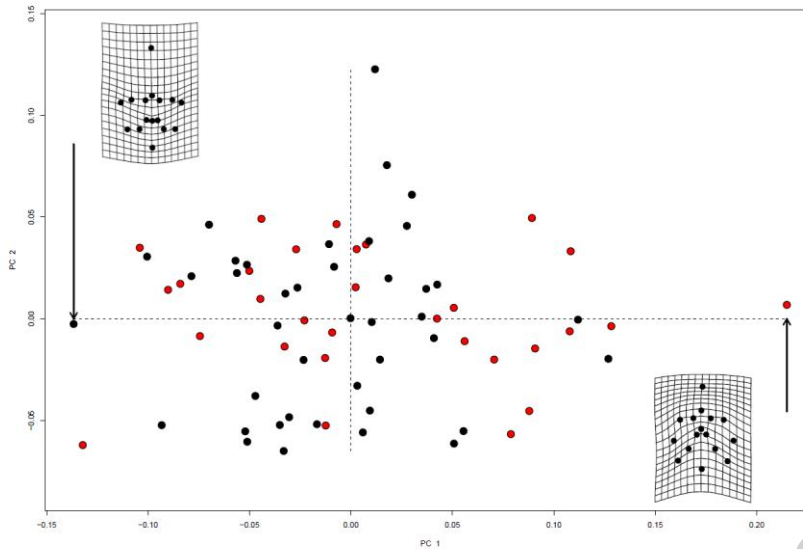


Figure 8. Principal components (such as the first principal component PC1, horizontal axis) represent the variance within the total population of deformed and control skull: for instance, PC1 represents 44.47% of the global variance. PC1 did not visually segregate deformed skulls (**black dots**) from control skulls (**red dots**). Negative PC1 values seemed to correspond to deformed skulls, with a lengthening of the face, and positive PC1 values seemed to correspond to the control group. Despite the apparent overlap of deformed and controls skulls along PC1, the two groups were significantly differentiated along this principal component, indicating that frontal views contained sufficient morphological information to discriminate deformed individuals from controls.

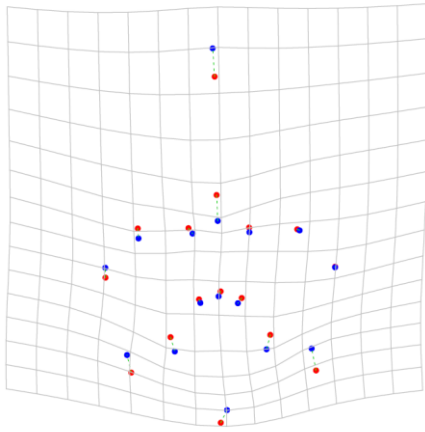


Figure 9. First canonical axis showing the global differences in frontal views between deformed skulls (**blue dots**) and control skulls (**red dots**). This visualization allows to map the main differences between mean representations of both groups, with indications on the deformations required to transform controls into Toulouse skulls, mostly corresponding to a lengthening of the face and a drop of the lip commissures.

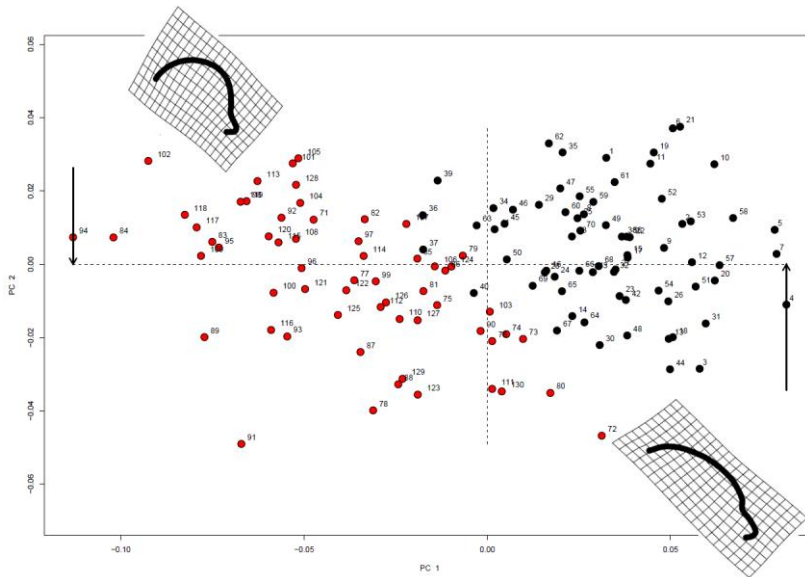


Figure 10. While the morphometric assessment of frontal views along PC1 did not visually discriminate deformed skulls from controls (Figure 8), for lateral views, the first principal component (PC1, horizontal axis) clearly separated deformed skulls (**black dots**) from control skulls (**red dots**). Positive PC1 values corresponded to the deformed group, with a lengthened and flattened skull vault.

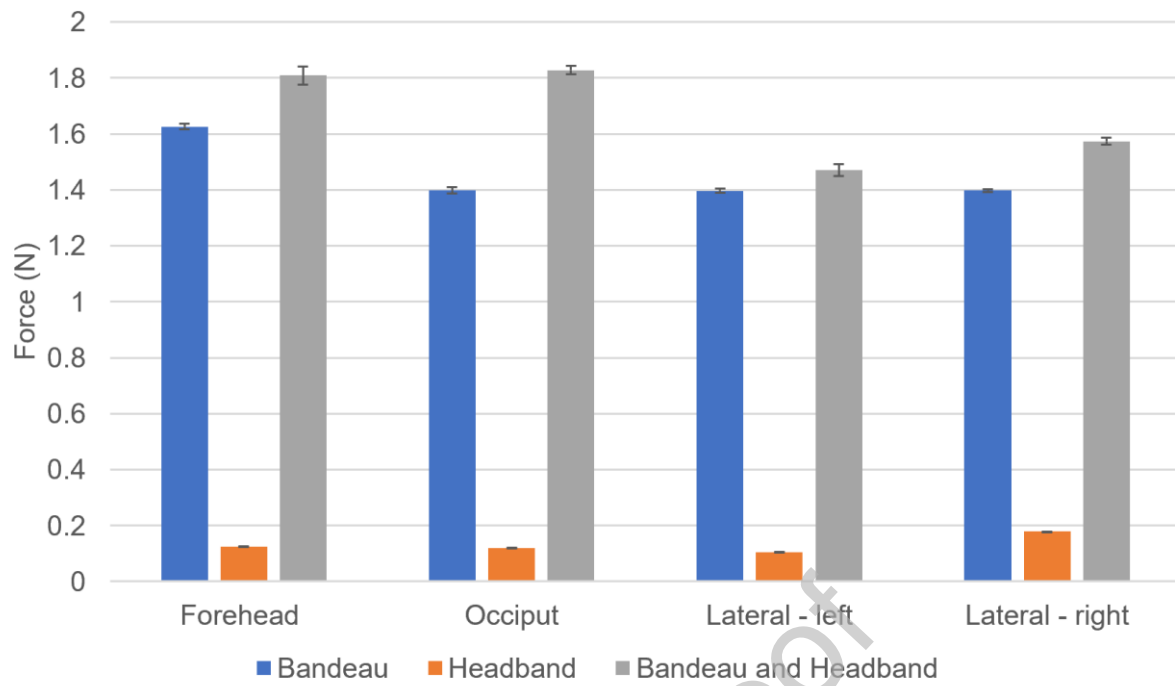


Figure 11. Forces exerted on the forehead and occiput by the headband and the bandeau on a 3D-printed newborn skull.

Table 1. Landmarks used in the morphometric analysis of frontal and lateral pictures.

Landmark		Definition	Type
Forehead top	1	Highest point of the forehead on the midline	midline
Glabella	2	Maximal inferior convexity of the forehead	midline
External canthus	3, 3'	External corner of the eye	bilateral
Internal canthus	4, 4'	Internal corner of the eye	bilateral
Tragion	5, 5'	Most anterior point of the supra-tragal concavity of the external ear	bilateral
Nasal prominence	6	Most anterior point of the tip of the nose	midline
Alare	7, 7'	Most external point of the convexity of the <i>alae nasi</i>	bilateral
Lip commissure	8, 8'	Junction between upper and lower lips	bilateral
Goniac angle	9, 9'	Angle between the posterior border of the ramus and the lower border of the body of the mandible	bilateral
Chin	10	Most inferior point of the mandibular symphysis	midline
Profile	Pf	From the vertex (in Frankfort orientation) to the columella	100 sliding landmarks

Table 2. Review of quantitative studies available in the literature on Toulouse deformations.

<i>Reference</i>	<i>Type of data</i>	<i>Cases</i>
Icart (1784)	Population study	NA
Coutelle (1808) (11)	Population study	NA
Foville (1834)	Review	NA
Bérenguier (1850)	Review	NA
Broca (1871) (5)	Autopsy	1
Broca (1879) (6)	Autopsy	1
Broca (1880)	Mould of brain cavity	1
Delisle (1880) ¹	Population study	NA
Delisle (1889) (15)	Photographs	4
Ambialet (1893) (2)	Autopsy	15
Delisle (1902) (16)	Population study	NA
Gourc (1913)	Population study	NA
Calvet (1964)	NA	NA
Fabié (1968)	2D morphometrics	18
Gélis (1984)	review	NA
Cussenot et al. (1992) (13)	2D morphometrics	1

¹ Delisle F. Contribution à l'étude des déformations artificielles du crâne. Thèse de Médecine, Paris, 1880. №154.

Janot et al. (1993) (33)	2D morphometrics	14 ²
Khonsari et al. (2013) (36)	3D morphometrics	7
Alary (2015)	NA	NA
Cottin et al. (2017) (10)	3D geometric morphometrics	7
Ketoff et al. (2017) (34)	3D geometric morphometrics	7
Sandy et al. (2018) (52)	3D geometric morphometrics	7
Current study	2D geometric morphometricss	101

² 10 voûtes, 4 crânes complets.

Table 3. Craniofacial repercussions of Toulouse deformations. *: controversial. After Coutelle, 1808; Foville, 1854; Gosse, 1855; Broca, 1871; Broca, 1879³; Delisle, 1880⁴; Delisle, 1889; Ambialet, 1893; Delisle, 1902; Gélis, 1984; Cussenot et al., 1992; Janot et al., 1993; Khonsari et al., 2013; Cottin et al., 2017; Ketoff et al., 2017; Sandy et al., 2019.

Anatomical region	Anomalies
Skull vault	<ul style="list-style-type: none"> - Low cranial index - Dura adherences - Irregular external surface - Thickness variations - Post-coronal groove* - Collateral venous circulation - Conserved intracranial volume
Skull base	<ul style="list-style-type: none"> - Platybasia - Medialisation of glenoid cavities* - Mastoid abrasion*
Brain	<ul style="list-style-type: none"> - Frontal retrusion following skull deformation
Orbits	<ul style="list-style-type: none"> - Sagittal shortness - Posterior pinch - Anterior opening - Conserved volumes

³Broca P. Crâne et cerveau d'un homme atteint de la déformation toulousaine. Bull Mem Soc Anthropol Paris 1879;2:417-420.

⁴Delisle F. Contribution à l'étude des déformations artificielles du crâne. Thèse de Médecine, Paris, 1880. №154.

Zygoma / maxilla	<ul style="list-style-type: none">- Zygomatic retrusion- Converved maxillary sinus volumes
Mandible	<ul style="list-style-type: none">- No prognathism*
External ear	<ul style="list-style-type: none">- Deformation and tissue loss
Craniofacial soft tissues	<ul style="list-style-type: none">- Hair loss and scars in compression zones

Journal Pre-proof